DESIGN AND CONSTRUCTION OF A LOW CAPACITY PUMP-LESS ABSORPTION SYSTEM

by

Hamed MONSEF*, Mohammad NAGHASH ZADEGAN, and Koroush JAVAHERDEH

Mechanical Engineering Department, University of Guilan, Rasht, Gilan, Iran

In this investigation, a low capacity absorption system has been designed and constructed where the mechanical pump has been replaced with a bubble pump, reducing the cost and eliminating the electrical power. Initially, a test rig bubble pump has been built with a single Pyrex tube to test the effect of different parameters on pumping flow rate. An absorption refrigeration system with a capacity of 2.5 kW has been designed and constructed. Results have shown that a bubble pump with five horizontal tubes with 2.5 mm diameter and submergence ratio of 0.4 has the best performance for this low capacity absorption refrigeration system. The COP of this structure was about 0.51 and mathematical modeling shows that increasing the solution concentration at generator outlet decreases the COP of the system.

Key words: *absorption system, bubble pump, LiBr, design and construction, refrigeration, horizontal tube*

Introduction

A conventional absorption refrigeration system is running primarily on heat energy, requiring a mechanical energy to circulate the refrigerant-absorbent solution from the absorber (low-pressure zone) to the generator (high-pressure zone). Due to the high cost of these types of mechanical pumps their use in residential consumption are costly. Platen and Munters [1] studied the absorption refrigerating cycle, where the circulation of the working fluids is carried out by a bubble pump. The advantages of their absorption refrigeration system are silent operation, no moving parts (fans or pumps) and portability.

Chen *et al.* [2] changed the generator configuration and increased the COP of the cycle and efficiency of the heating process with reduction of heat losses at cycle. The generator consists of heating elements, a bubble pump and a coaxial heat exchanger. Pfaff *et al.* [3] developed a mathematical model to evaluate the bubble pump's performance. A test rig has been made to validate the mathematical model and to evaluate the bubble pump performance. They have found that the bubble pump operated at slug flow regime in cyclic intervals. They have shown that the ratio between the strong LiBr solution flow rate and the refrigerant flow rate (water vapor) is independent of the heat input.

---

* Corresponding author; e-mail: hamed.monsef@gmail.com

Delano [4, 5] analyzed the Einstein refrigeration cycle; the cycle used a bubble pump to circulate the working fluids. He developed an analytical model to appraise the bubble pump performance. The analytical model has been used to investigate the influence of heat input, tube diameter and submergence ratio on bubble pump performance. Delano found that increasing the heat input to the bubble pump for a fixed submergence ratio, increases the flow rate of the liquid through the bubble pump to a maximum value where a further increase in the heat input, decreases the liquid flow rate. He showed that increasing the tube diameter increases the flow rate through the bubble pump.

White [6] presented another analytical model using an air-lift pump theory for the bubble pump. The model was developed based on mass and momentum conservation equations. An experimental test rig was built using an air-lift pump to analyze the bubble pump performance and validate the model. She found that if the bubble pump operates at slug flow regime the analytical model is reliable.

Koyfman *et al*. [7] presented a bubble pump that operates continuously. The flow was pumped by boiling of a binary mixture (as in a real diffusion absorption refrigerating unit). Koyfman *et al*. [8] also presented an experimental investigation was undertaken to study the performance of the bubble pump for diffusion absorption refrigeration units.

In this research the design and performance of a LiBr refrigeration system were investigated while the mechanical pump was replaced with a bubble pump. The operation and performance of the system has also been analyzed.

Bubble pump

A bubble pump is a thermal fluid pump, using thermal energy to pump liquid from lower level to the higher level as shown in fig. 1. The generated small bubbles at the bottom of the pump tube join and form bigger vapor bubbles. The rising vapor bubble acts like a piston and lifts a corresponding liquid slug to the top of the bubble pump tube. The bubble pump operates most efficiently in the slug flow regime in which the diameter of vapor bubbles is approximately the same of diameter of the tube. The four basic flow patterns observed in vertical two phase flows are bubbly, slug, churn, and annular as shown in fig. 2. [9]
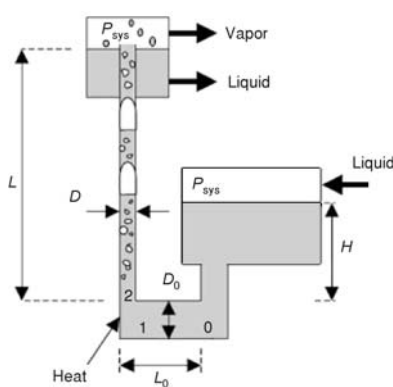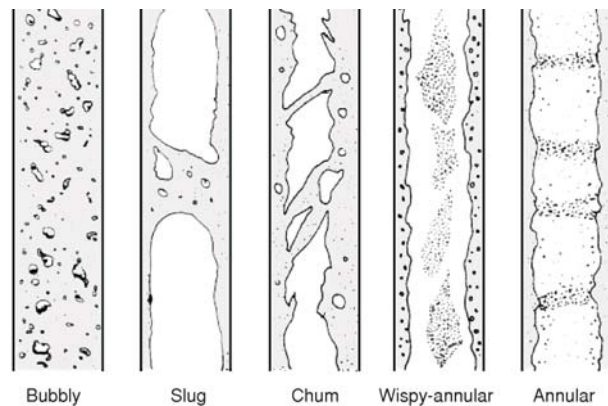

Figure 1. A schematic of bubble pump

Figure 2. Different flow regime in bubble pump

Monsef, H., *et al.*: Design and Construction of a Low Capacity Pump-Less ...
THERMAL SCIENCE: Year 2014, Vol. 18, No. 2, pp. 577-590

579

Theory

The submergence ratio of the bubble pump describes the average pressure gradient along the lift tube. This parameter expressed in terms of velocities, fluid properties, and geometrical parameters. The governing equations are based on fig. 1. The following assumptions have been made:
- the frictional losses in the entrance of the lift tube have been neglected, and
- the change in momentum throughout the left tube has been neglected.

Momentum equation from P_{sys} to 0 gives:

$$P_0 = P_{sys} + \rho_L g(H) - \rho_L \frac{V_0^2}{2} \tag{1}$$

Momentum equation from point 0 to 1 (neglecting friction) gives:

$$P_1 = P_0 - \rho_L V_0 (V_1 - V_0) \tag{2}$$

Conservation of mass from point 0 to 1 yields:

$$\rho_L A_0 V_0 = \rho_L A_1 V_1 \tag{3}$$

Since $A_0 = A_1$, therefore:

$$V_0 = V_1 \tag{4}$$

Momentum equation from point 1 to 2 yields (neglecting friction):

$$P_2 = P_1 - \rho_H V_1 (V_2 - V_1) \tag{5}$$

where ρ_H is the homogeneous density of the two-phase flow. The velocities of liquid and vapor in the region between point 1 and 2 are approximately equal; therefore a homogeneous density is used in this momentum equation. The expression for the homogeneous density can be found from the conservation of mass from 1 to 2. Conservation of mass from state 1 to 2 for the experimental air-lift pump set-up yields:

$$\rho_1 A_0 V_1 + \dot{m}_G = \rho_H A_2 V_2 \tag{6}$$

Since $A_2 = \pi D_2^2/4$, $D_2 = D$ also having liquid at point 1:

$$\rho_H = \frac{\rho_L D_0^2 V_1 + \dfrac{4}{\pi} \dot{m}_G}{D^2 V_2} \tag{7}$$

The homogeneous density is obtained by eliminating the gas mass flow rate in eq. (7):

$$\rho_H = \frac{\rho_L D_0^2 V_1}{D_2^2 V_2} \tag{8}$$

At this point, the two-phase flow terminology is needed to proceed because the flow in the lift tube is most clearly defined in these terms. The definitions of superficial velocities and void fraction can be related to the terminology used.

Points 0 and 1 are under liquid conditions. Therefore:

$$V_0 = V_1 = \frac{\dot{\forall}_L}{A_0} \tag{9}$$

580

Monsef, H., *et al.*: Design and Construction of a Low Capacity Pump-Less ...
THERMAL SCIENCE: Year 2014, Vol. 18, No. 2, pp. 577-590

while the definition of j_L is:

$$j_L = \frac{\dot{\forall}_L}{A} \tag{10}$$

Therefore:

$$V_0 = V_1 = j_L \left(\frac{A_t}{A_0} \right) \tag{11}$$

V_2 describes the total average velocity of the mixture:

$$V_2 = \frac{\dot{\forall}_L + \dot{\forall}_G}{A_t} = \frac{\dot{\forall}}{A_t} \tag{12}$$

This is precisely the definition of j. Therefore:

$$V_2 = j \tag{13}$$

Manipulating eqs. (11) and (13) give:

$$V_2 - V_1 = j - j_L \left(\frac{A_t}{A_0} \right) \tag{14}$$

The void fraction is defined as the average cross-sectional area occupied by the gas divided by the total cross-sectional area of the tube. Therefore:

$$\frac{A_L}{A_t} = \frac{A_t - A_G}{A_t} = 1 - \varepsilon \tag{15}$$

The momentum equation in the lift tube (from state 2 to P_{sys}) can be stated as [6]:

$$P_2 = P_{sys} + f_{TP} \frac{(\rho_L j_L + \rho_G j_G)^2}{2\rho_{TP}} \left(\frac{L}{D} \right) + \rho_L L_g (1 - \varepsilon) \tag{16}$$

Here f_{TP} is the two-phase friction factor (based on average properties of liquid and gas) and ρ_{TP} – the two-phase density of the fluid mixture in the lift tube. Because there is no slip between the two phases, a two-phase density for the frictional pressure drop term is required instead of a homogeneous one. This two-phase density can be found by the density definition applied to the lift tube volume:

$$\rho_{TP} = \rho_G \varepsilon + \rho_L (1 - \varepsilon) \tag{17}$$

a general equation for the submergence ratio (H/L), describing the average pressure gradient along the lift tube can be obtained by manipulating eqs. (1), (2), (4), (5) and (16) [6]:

$$\frac{H}{L} = \frac{f_{TP}(\rho_L j_L + \rho_G j_G)^2}{2gD\rho_L\rho_{TP}} + \frac{j_L^2 \left(\dfrac{D}{D_0} \right)^4}{2gL} + \frac{j_L \rho_H \left(\dfrac{D}{D_0} \right)^2 \left[j - j_L \left(\dfrac{D}{D_2} \right)^2 \right]}{\rho_L gL} + (1 - \varepsilon) \tag{18}$$

To observe the actual effects of diameter, submergence ratio and input heat, an experimentally single pipe Pyrex bubble pump has been built and tested with various diameters, submergence ratio (H/L) and input heat to find the best structure in an absorption system. The experimental results of the single pipe Pyrex bubble pump are shown at fig. 3 through 5. Figure 3 shows the vapor flow rate from bubble pump *vs.* internal heat power for different pipe diameters.

The vapor flow rate increases to a maximum value as the input heat increases, reaching a constant value at about 800 W where the flow regime has been changed to churn and annular
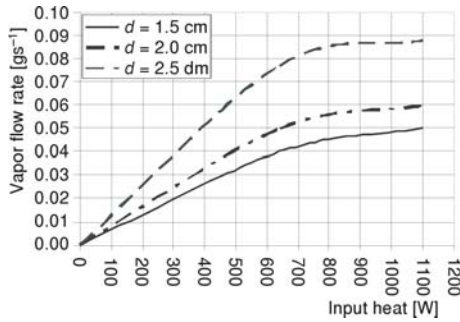
Monsef, H., *et al*.: Design and Construction of a Low Capacity Pump-Less ...
THERMAL SCIENCE: Year 2014, Vol. 18, No. 2, pp. 577-590

581

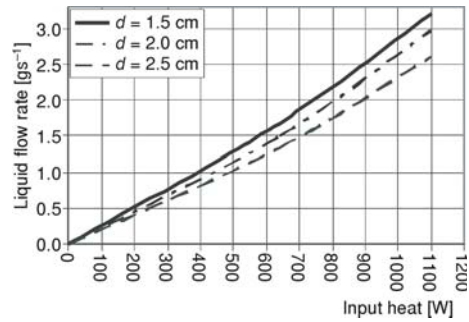**Figure 3. Variation of vapor flow rate *vs*. internal power**

Figure 4. Variation of liquid flow rate *vs*. internal heat power

from slug regime [10]. Results of Pyrex bubble pump experiments show the larger tubes have more vapor flow rate for the same input heat. Figure 4 shows the variation of liquid flow rate *vs*. the input heat.

It is seen when the input heat increases, the liquid flow rate increases too. The results show that the liquid flow rate in the smaller tubes is more than that of the larger tubes. For smaller tubes, the bubbles fill the tubes easily and push the fluid upward, acting like a piston.

Figure 5 demonstrates the effect of submergence ratio (*H/L*) on the liquid flow rate. The figure shows that the larger *H/L* has the larger liquid flow rate. At *H/L* less than 0.2 the bubbles reach to the surface of fluid rapidly. Because enough fluid does not exist between the bubbles therefore the fluid could not be lift upward.

The experimental results show that, the vapor flow rate is increased in larger tubes than that of the smaller tube. Therefore the larger tubes in bubble pump are more desirable. The liquid flow rate also must be adequate to absorb the refrigerant at the absorber; therefore the tube diameter should be selected appropriately.

The performance of absorption systems with bubble pump is exactly similar to the performance of systems with a mechanical pump, where bubble pump increases the pressure of fluid and circulate the fluid in the cycle. Figure 6 shows a schematic diagram of a LiBr absorption system using a bubble pump.
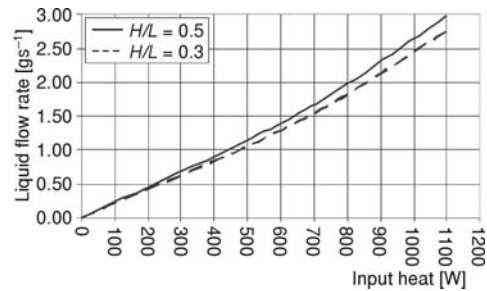

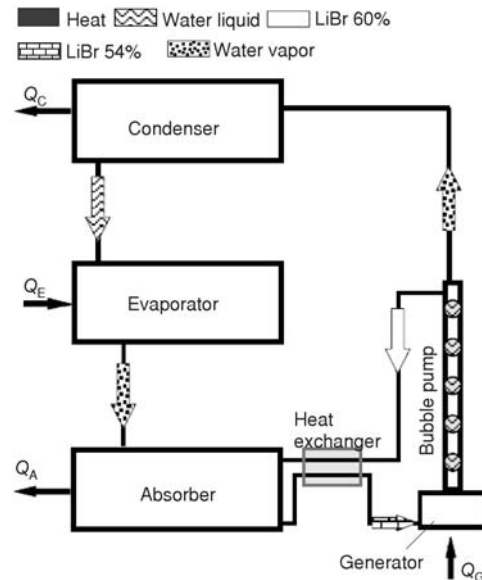**Figure 5. Effect of submergence ratio (*H/L*) on liquid flow rate**

Figure 6. A schematic diagram of a LiBr absorption system with bubble pump

Experimental set-up

To build an absorption refrigerant system with low capacity, the amount of refrigerant (water) at evaporator should be calculated. Equation 19 calculates the amount of water circulating ($\dot{m}_R$) in the system:

$$\dot{Q}_e = \dot{m}_R h_{fg} \tag{19}$$

Because of U-shape tube performance at this state, the quality of water entering to evaporator was zero.

For a system with capacity of 2.5 kW , the required water flow rate is about 1.075 g/s (properties of materials obtained from EES* library). Experimental results show that a bubble pump with five tubes of 2.5 cm diameter and $H/L = 0.4$ can produce this flow rate.

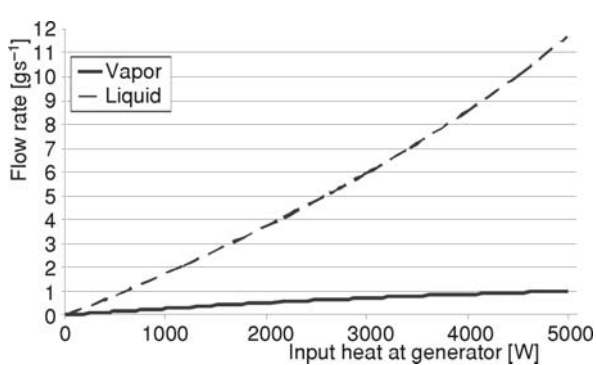A five-tube steel bubble pump has been made. The generator and bubble pump are united in this system. Figure 7 shows the vapor and liquid of LiBr solution flow rates for the bubble pump. The principle flow regime at this pump is slug regime. Experiments show the governing flow regime in larger tubes will be annular and adequate liquid cannot flow to the absorber.

Figure 7. Flow rate of vapor and strong LiBr
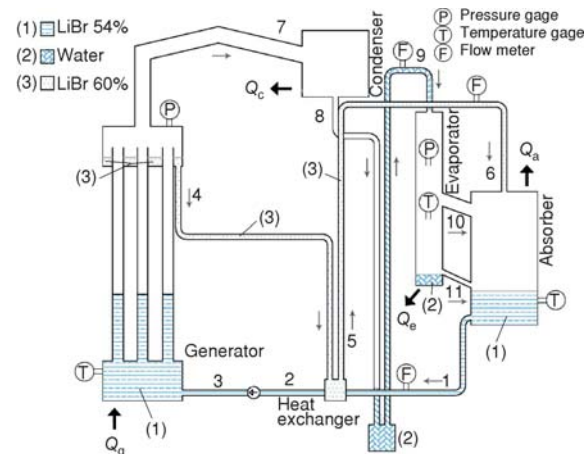
Figure 8. Schematic of built absorption refrigeration system

Vertical tubes with low inner friction are used to increase the efficiency of pump. The heat transfer between bubbles and surrounding fluid will reduce the size of bubbles where small bubbles can not lift above the fluid and bubbles will finally be exploded.

Increasing density of strong solution increases the absorbed vapor in the absorber, but the high density of solution can cause crystallization of strong solution in the absorber.

Increasing input heat in generator increases the pressure of the condenser which has two disadvantages:
– The pumping of LiBr solution will be reduced, because the pressure at upper tank will be increased.
– Increasing pressure of the condenser will stop refrigeration cycle due to disturbed pressure balance in the cycle. Thus the input heat in generator must have an optimum amount. Figure 8 shows the absorption refrigeration system test rig.

* Engineering equation software ®

Condenser

A shell and tube condenser is used where vapor flows in the shell and cooling fluid flows in copper tubes. The condenser performance is given by energy equilibrium (fig. 8).

$$\dot{Q}_{con} = m_7 (h_7 - h_8)$$

(20)

The total heat transfer rate ($\dot{Q}$) can be determined from the expression:

$$\dot{Q} = A U \Delta T_m$$

(21)

where

$$\Delta T_m = F \Delta T_{ln} = F \left(\frac{\Delta T_0 - \Delta T_L}{\ln\left(\dfrac{\Delta T_0}{\Delta T_L}\right)} \right)$$

(22)

The overall heat transfer coefficient (U) based on the outside surface of the tube is defined as [11]:

$$U = \frac{1}{\dfrac{D_o}{D_i}\dfrac{1}{h_i} + \dfrac{D_o}{D_i}F_i + \dfrac{1}{2k}D_o \ln\dfrac{D_o}{D_i} + F_o + \dfrac{1}{h_o}}$$

(23)

The value of the fouling factors (F_i, F_o) at the inside and outside surfaces of the tubes can be taken as 0.09 m^{2}K/kW [12]. For a copper heat exchanger, k can be calculated by curve fitting method [11]. Equation 23 has been used in a computer program for designing the shell and tube condenser. For this research, the cooling water inlet and outlet temperatures must be assumed as input value.

Assuming a turbulent flow, the heat transfer coefficients (h_o, h_i) for the inside and outside flow is given by [13]:

$$\overline{Nu}_D = \frac{\dfrac{f}{8} Re_D Pr}{K_1 + K_2 \sqrt{\dfrac{f}{8}}(\sqrt[3]{Pr^2} - 1)}$$

(24)

where $f = (1.82 \log_{10} Re_D - 1.64)^{-2}$, $K_1 = 1 + 3.4 f$, and $K_2 = 11.7 + (1.8 Pr^{1/3})$.

Equation (24) applies for $10^4 < Re_D < 5 \cdot 10^6$ and $0.5 < Pr < 2000$, respectively.

The water properties are evaluated at a mean temperature. Nusselt's analysis of heat transfer for condensation on the outside surface of a horizontal tube gives the average heat transfer coefficient as [14]:

$$h_m = 0.725 \left[\frac{g\rho_1 (\rho_1 - \rho_v)h_{fg}k_l^3}{\mu_1 (T_v - T_w)D_o} \right]^{-0.25}$$

(25)

The logarithmic mean temperature difference has been used to evaluate the necessary heat transfer area of the tubes.

Solution heat exchanger

One of most important points to increase the efficiency of the system is selecting a suitable heat exchanger. The heat exchanger warms the weak solution, coming from absorber,

reducing temperature of strong solution coming from bubble pump before entering to absorber. Lower temperature of strong solution helps to absorb vapor easier.

Equation (23) is used to calculate the overall heat transfer coefficient. The value of the fouling factors (F_i, F_o) for the inside and outside surfaces of the tube are taken as 0.09 m²K/kW [12] and k for copper will be evaluated at a mean temperature. The heat transfer coefficients h_o, h_i for the inside and outside flow are determined as follows.

The LiBr solution properties at a mean temperature are calculated and the Reynolds number is determined from:

$$\text{Re} = \frac{4\dot{m}}{\pi D \mu} \tag{26}$$

where μ is the viscosity of LiBr solution, calculated by eq. (31). For laminar flow, the Nusselt number is given [12]:

$$\text{Nu} = \frac{h_i D_i}{k} = 3.66 \tag{27}$$

The Reynolds number based on the hydraulic diameter (D_H) and the bulk temperature properties is:

$$\text{Re} = \frac{\rho V \overline{D_H}}{\mu} = \frac{\dot{m} D_H}{4\mu} \tag{28}$$

For laminar flow, as before Nu = $h_o D/k$ = 3.66 [15], and therefore, h_o will be evaluated.

By substituting the values in eq. (23), the overall heat transfer coefficient (U) based on the outside surface of the tube is subsequently evaluated.

Finally the logarithmic mean temperature can be calculated, and the area of the heat exchanger will be determined, eq. (21).

Evaporator

Evaporator has been designed similar to condenser where the external heat transfer coefficient should be calculated by Jacob-Havkings formula [16]:

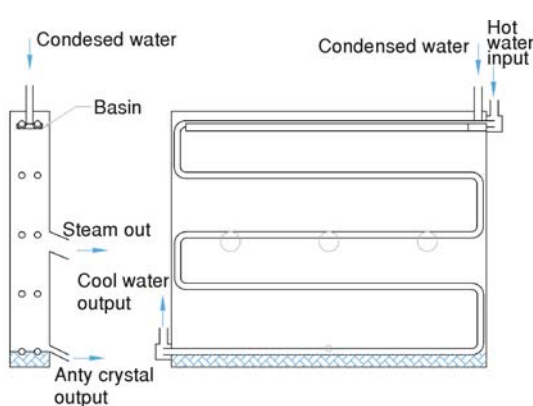$$h_o = h_1 \left(\frac{P}{P_1} \right)^{0.4} \tag{29}$$

Figure 9. Side and front view of designed evaporator

Here P is the evaporator pressure, P_1 – the atmospheric pressure, and h_1 – the convection coefficient in atmospheric pressure. Results have shown a 0.4 m² of copper surface for system's evaporator is necessary. One of the most important parameters in evaporator is the contact area between condensed water (from condenser) and copper tubes. For this reason a basin is used to shower water on the parallel tubes.

The velocity of water particles within tubes is important; therefore, the distance between parallel tubes has been increased to increase the velocity of water. Figure 9 shows a designed evaporator sketch.
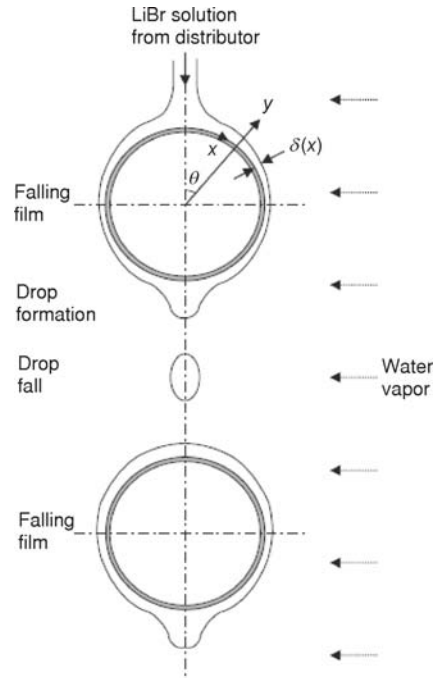
Absorber

In an absorber, the strong solutions, coming from bubble pump, absorb water vapor coming from the evaporator. In a recent study, a model for absorption of water vapor into aqueous LiBr flowing over a horizontal smooth tube was developed. The flow regimes at absorber are divided into three like the Kirby [17] model:
–   falling film in contact with the tube,
–   drop formation at the bottom of the tube, and
–   drop fall between the tubes.

Figure 10 shows three governing regimes in strong LiBr solution on copper tubes.

Kyung *et. al* [18] developed a model for absorption of water vapor into aqueous LiBr flowing over a horizontal smooth tube. The results have been used to build an absorber for this research.

Figure 11 shows a sketch and a schematic of construction absorber. As in the evaporator, a basin was used for pouring strong LiBr solution on the horizontal tubes so that it can easily absorb water vapor coming from the evaporator.

Figure 10. Three applied regime of strong solution of LiBr on horizontal tube
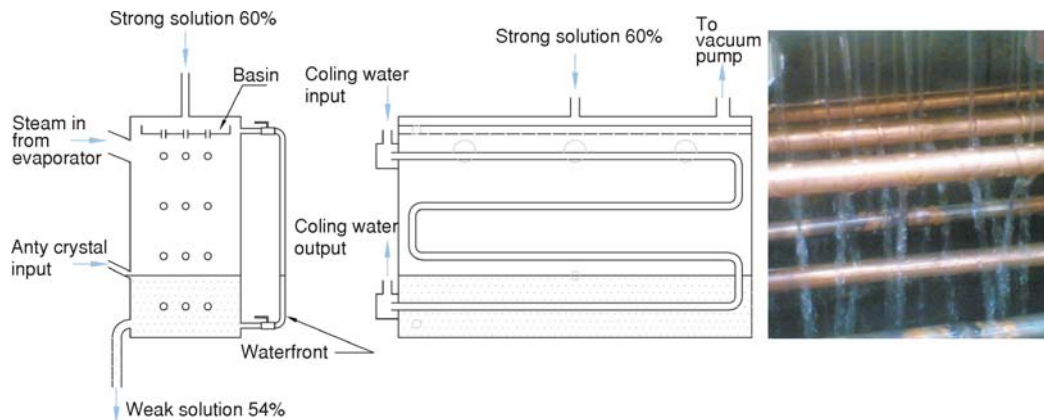
Figure 11. (a) Sketch of absorber from two visages; (b) Falling solution on absorber horizontal tubes

Figure 12 shows a schematic of the experimental system built at Guilan University with capacity of 2.5 kW . The machine was built with steel and a vacuum pump has been used to decrease the system pressure before testing. Manual and digital gages were installed in the system to measure temperature and pressure at all points of the system.
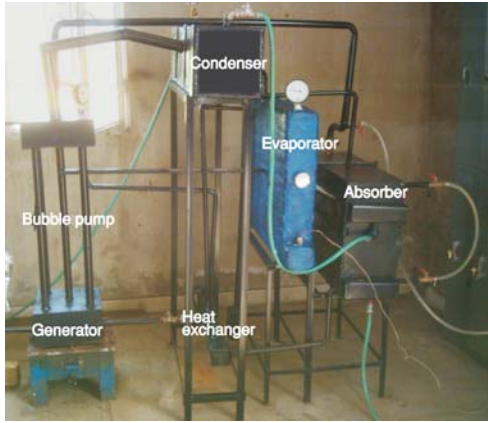
586

Monsef, H., *et al.*: Design and Construction of a Low Capacity Pump-Less ...
THERMAL SCIENCE: Year 2014, Vol. 18, No. 2, pp. 577-590

Figure 12. Schematic of built refrigeration absorption system

The cycle works at two levels of pressures (0.93 kPa and 9.66 kPa). When the pressures are matched, the refrigerant system will work properly. In this system, a U-shape tube was used between the condenser and the evaporator and also another U-shape tube was used between the absorber and the bubble pump. The pressure difference is 8.73 kPa, where a U-shape tube with 90 cm heights produces such a pressure difference between the condenser and the evaporator. Although due to density of LiBr solution, a U-shape tube with 55 cm heights could produce this pressure difference too. The density of strong LiBr solution in this point is given by eq. (30) which is about 1600 kg/m³:

– density of LiBr solution [19]

$$\rho_x[\text{kgm}^{-3}] = 1145.36 + 470.48 X_0 + 1374.79 X_0^2 - (0.333393 + 0.571749 X_0)(273 + T)$$

$$\text{Range } 20\% < X < 60\% \text{ LiBr}$$

$$X_0 = \frac{X}{100} \tag{30}$$

$$T = \text{solution temperature } [° \text{C}], \text{ range } 0 < T_{sol} < 200$$

– viscosity of LiBr solution [19]

$$\mu_x[\text{kgms}^{-1}] = e^B/1000$$

$$\text{Range } 40\% < X < 70\% \text{ LiBr}$$

$$A_1 = -494.122 + 16.396 X - 0.1451 X^2, \; A_2 = 28606.4 - 934.569 X + 8.527 X^2 \tag{31}$$

$$A_3 = 70.384 - 2.350 X + 0.020 X^2, \; B = A_1 + \left(\frac{A_2}{TK}\right) + A_3 \ln(TK)$$

$$TK = \text{solution temperature [K]}$$

A one-way valve was used between absorber and generator which prevents bubbles returning to the absorber, at the start of pumping. Since the volume of generator is fixed, as soon as some solution pumped, it will be vacuumed and let the weak solution to be pulled from absorber to generator.

The fluid in the bubble pump has not been pumped continuously, because after completing the first cycle, it takes time to heat the solution and produce bubbles. Because the system's pressure is too low comparing with that of atmospheric pressure, these periods are too short and the fluid is pumped highly intermittently.

To find suitable conditions for specific applications, a sensitivity analysis can be performed utilizing a computer program, which follows the mathematical correlations. The simulation's results show the effect of T_3 and T_5, (T_3 is the temperature of input weak LiBr solution to the generator, where T_5 is the temperature of input strong LiBr solution to the absorber) and outlet solution concentration from absorber on system's *COP* (fig. 13). Increasing the outlet solu-

tion concentration, coming from the absorber decreases *COP*, because strong solution couldn't absorb necessary vapor at the absorber. The graph shows a higher concentration more than 56% causes a decrease of *COP* to less than 0.5. Results also show that increasing T_3 can increase *COP* of system because of the lower energy consumed at generator to boil weak solution. Decreasing T_5 also can increase *COP* because of a lower temperature strong solution can absorb water vapor better.
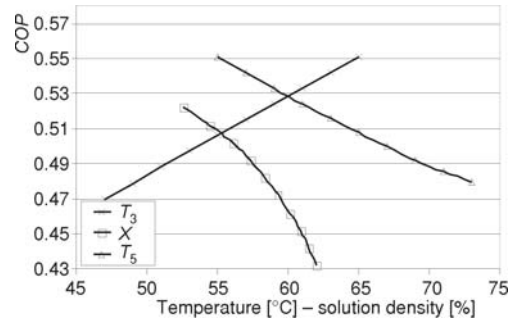
Experimental results

The experimental results are shown in tabs. 1 and 2. The results are in a good agreement with results of Florides *et al*. [15].

Figure 13. Effect of T_3, T_5, and outlet solution density from absorber on *COP*

Table 1. Fluid state in different point of cycle (points shown in fig. 9)

Point	$\dot{m}$ [gs^{-1}]	P [kPa]	T [°C]	X [%LiBr]
1	12.1	0.93	35	54
2	12.1	0.93	55	54
3	12.1	9.66	55	54
4	11.03	9.66	85	59
5	11.03	9.66	65	59
6	11.03	0.93	65	59
7	1.075	9.66	80	0
8	1.075	9.66	42	0
9	1.075	0.93	6	0
10	1	0.93	6	0
11	0.075	0.93	6	0

Table 2. Heat balance of different part of cycle

Description	Symbol	kW
Capacity (evaporator output power)	$\dot{Q}_e$	2.5
Absorber heat, rejected to the environment	$\dot{Q}_a$	3.6
Heat input to the generator	$\dot{Q}_g$	4.9
Condenser heat, rejected to the environment	$\dot{Q}_c$	2.8
Coefficient of performance	*COP*	0.51

The data has been read from *K* kind thermocouples, temperature and pressure gages and solution flow meters. The rate of heat in the evaporator, the condenser and the absorber has been measured with the temperature difference between the inlet and the outlet solution. The concentration of LiBr solution has been measured by a density meter bulb where the input heat in the generator has been measured by an internal energy of natural gas and its flow rate. A calibration procedure was applied to all instruments described in fig. 8. Using the calibration functions for every sensor, the systematic errors were reduced as far as possible. The random uncertainty (*U*) for an experimental result (*R*), which is function of *n* independent parameters (x_i), is estimated, according to a Gaussian statistics based algorithm [20].

$$U = \sqrt{\sum_{i=1}^{n}\left(\frac{\partial R}{\partial x_i} U_{xi} \right)^2}; \quad R = f(x_1, x_2, \dots x_n) \tag{32}$$

588

Monsef, H., *et al.*: Design and Construction of a Low Capacity Pump-Less ...
THERMAL SCIENCE: Year 2014, Vol. 18, No. 2, pp. 577-590

The uncertainty of instruments is given in tab. 3. For the cases of thermocouples and pressures sensors, the uncertainty ranges given corresponds to a minimum and maximum value for the whole set of calibrated instruments.

Table 3. Sensors used in experimental test rig

Instrument	Quantity	Range	Uncertainty
Temperature gages	3	0-120 °C	±(0.2 °C-0.8 °C)
Thermocouple	1	0-1200 °C	±0.5 °C
Pressure gages	2	−1-0 bar	±(1.8-2.5)%
Strong solution flow meters	1	20-70 kg/h	±2.7%
Refrigerant flow meters	1	2-7 kg/h	±3.1%
Neutral gas flow meter	1	0.2-1 m³/h	±4.2%
LiBr density meter	1	0-100 %	±0.8%

Low pressure of generator causes weak solution to boil in low temperature (in atmosphere pressure it boils in 145 °C but here it boils in 80 °C). High concentration of strong solution can absorb vapor of air, causing more water to be vaporized in the evaporator. One of the big problems of LiBr low capacity refrigeration system is water type condenser. These types of condensers need cooling tower which is for residential consumption, unacceptable. The low pressure does not allow use of air cooled condensers because the amount of pressure is not enough to overcome the friction power in the condenser pipes in air type condenser.

Conclusions

In this research, a test rig bubble pump was built using a single tube to find the best diameter and submergence ratio for use in absorption systems. According to the primary results, a bubble pump with five steel vertical tubes was built which was used in a low capacity (2.5 kW) absorption system. At this system, the bubble pump was combined with the generator. An evaporator, absorber, condenser, and a heat exchanger have also been designed and constructed. The bubble pump and the generator's shape play an important role in the *COP* of the system. Bubble pump of the system has to be tested to find the liquid and the vapor flow rate for each new sketch for other capacities. Generator input heat is almost an important parameter to balance the cycle pressure and pumping solution.

The electrical energy has not been used in this system; therefore where this energy has high cost, it is more affordable. Because the temperature of generator is about 80 °C, it may utilize low potential heat sources, such as solar energy, to operate the cycle. Calculations have shown the primary cost of this system is lower than ordinary absorption refrigeration systems.

Acknowledgment

Nomenclature

A – surface of absorption system's heat exchanger, [m^2]

A_t – total cross-sectional area of bubble pump's tubes, (= $\pi D^2/4$), [m^2]

Monsef, H., *et al.*: Design and Construction of a Low Capacity Pump-Less ...
THERMAL SCIENCE: Year 2014, Vol. 18, No. 2, pp. 577-590

589

A_G – cross-sectional area of bubble pump's tube (gas side), [m^2]

A_L – cross-sectional area of bubble pump's tube (liquid side), (= $A_t - A_G$), [m^2]

D – diameter of lift tube, [m]

D_i, D_o – inside and outside diameters of tube, respectively, [m]

F – correction factor depending on type of the heat exchanger

F_i, F_o – fouling factors at inside and outside surfaces of tube, [m^{2}KW^{-1}]

f – friction factor

f_{TP} – two-phase friction factor

g – gravitational acceleration, [ms^{-2}]

h_{fg} – latent heat, [kJkg^{-1}]

h_i, h_o – heat transfer coefficients for inside and outside flow, [W/m^{2}K]

h_m – average heat transfer coefficient, [Wm^{-2}K^{-1}]

H/L – submergence ratio

j – total average velocity of flow, (= $j_L + j_G$), [ms^{-1}]

j_G – gas superficial velocity, (= $\forall_G/A$), [ms^{-1}]

j_L – liquid superficial velocity, (= $\forall_L/A_t$), [ms^{-1}]

k – thermal conductivity, [Wm^{-1}K^{-1}]

$\dot{m}$ – total mass flow rate, [kgs^{-1}]

$\dot{m}_G$ – mass flow rate of gas, [kgs^{-1}]

Nu_D – Nusselt number

P – pressure, [Pa]

Pr – Prandtl number

Q – heat flow rate, [kW]

Re – solution Reynolds number for vertical tube

Re_D – Reynolds number

S – slip ratio between phases, (V_G/V_L)

ΔT_{ln} – logarithmic mean temperature difference, [K]

ΔT_m – mean temperature difference, [K]

ΔT_0 – temperature difference between hot and cold fluid at inlet, [K]

ΔT_1 – temperature difference between hot and cold fluid at outlet, [K]

t_v – vapor saturation temperature, [°C]

t_w – wall surface temperature, [°C]

U – average overall heat transfer coefficient, [Wm^{-2}K^{-1}]

V_G – velocity of the gas, (= j_G/ε), [ms^{-1}]

V_L – velocity of the liquid, [= $J_L/(1-\varepsilon)$], [ms^{-1}]

X_0 – percentage of LiBr solution

x – quality, ($\dot{m}_G/\dot{m}$)

$\forall_G$ – gas volumetric flow rate, [m^{3}s^{-1}]

$\forall_L$ – liquid volumetric flow rate, [m^{3}s^{-1}]

$\forall$ – total volumetric flow rate, (= $\forall_L + \forall_G$), [m^{3}s^{-1}]

Greek symbols

ε – gas void fraction of the flow, (= A_G/A_t)

μ – dynamic viscosity, [Nsm^{-2}]

μ_1 – absolute viscosity of liquid, [Nsm^{-2}]

v – kinematic viscosity, [m^{2}s^{-1}]

ρ – density, [kgm^{-3}]

ρ_1 – liquid density, [kgm^{-3}]

ρ_v – vapor density, [kgm^{-3}]

ρ_{TP} – two-phase density

References

[1] von Platen. B. C, Munters, C. G, Refrigerator, US Patent 1, 1928, pp. 685-764

[2] Chen, J., *et al*., Performance Enhancement of a Diffusion-Absorption Refrigerator, *International Journal of Refrigeration, 19* (1996), 3, pp. 208-218

[3] Pfaff, M., *et al*., Studies on Bubble Pump for a Water-Lithium Bromide Vapor Absorption Refrigeration, *International Journal of Refrigeration, 21* (1998), 6, pp. 452-462

[4] Delano, A. D., Analysis of the Einstein Refrigeration Cycle, M. Sc. thesis, Georgia Institute of Technology, Atlanta, Ga., USA, 1997

[5] Delano, A. D., Design Analysis of the Einstein Refrigeration Cycle, Ph. D. thesis, Georgia Institute of Technology, Atlanta, Ga., USA, 1998

[6] White, S. J., Bubble Pump Design and Performance, M. Sc. thesis, Georgia Institute of technology, Atlanta, Ga., USA, 2001

[7] Koyfman, A., *et al*., A Study on Bubble Pump Performance for Diffusion Absorption Refrigeration System with Organic Working Fluids, *Proceedings*, 2nd International Heat Powered Cycles Conference, Paris, 2001, pp. 81-86

[8] Koyfman, A., *et al*., An Experimental Investigation of Bubble Pump Performance for Diffusion Absorption Refrigeration, System with Organic Working Fluids, *Applied Thermal Engineering, 23* (2003), 15, pp. 1881-1851

[9] Collier, J. G., Thome, J. R., *Convective Boiling and Condensation*, McGraw-Hill Book Co., New York, USA, 1996

590

Monsef, H., *et al.*: Design and Construction of a Low Capacity Pump-Less ...
THERMAL SCIENCE: Year 2014, Vol. 18, No. 2, pp. 577-590

[10] Rohi, S., *et al.*, Experimental Analysis of Bubble Pump LiBr Solution Working Fluids for Absorption Refrigeration System, *Proceedings*, Eurosim, Ljubljana, Slovenia, 2007, pp. 366-371

[11] Ozisik, M., Boiling and Condensation, in: *Heat transfer – a Basic Approach*, McGraw-Hill Co., New York, USA, 1985

[12] Howell, R. H., *et al*., Refrigeration Equipment, in: *Principles of HVAC*, ASHRAE, Trans., 1998, pp. 505-534

[13] Kreith, F., Bohn, M. S., *Principles of Heat Transfer*, 5th ed. PWS Publishing Company, Boston, Mass., USA, 1997

[14] Ozisik, M., Heat Exchangers, in: *Heat Transfer – a Basic Approach*, McGraw-Hill Book Co., New York, USA, 1985, pp. 476-519

[15] Florides, G.A., *et al*., Design and Construction of a LiBr-Water Absorption Machine, *Energy Conversion and Management, 44* (2003), 15, pp. 2483-2508

[16] Jakob, M., Hawkings, G., *Elements of Heat Transfers*, 3rd ed., John Wiley & Sons, New York, USA, 1957

[17] Kirby, M. J., A Computational Model of Falling Film Absorption in Horizontal Tube LiBr Absorbers, M. Sc. thesis, The Pennsylvania State University, University Park, Penn., USA, 1995

[18] Kyung, I., *et al*., Model for Absorption of Water Vapor into Aqueous LiBr Flowing over a Horizontal Smooth Tube, *International Journal of Refrigeration, 30* (2007), 4, pp. 591-600

[19] Lee, R. J., *et al*., Properties of Lithium Bromide-Water Solutions at High Temperatures and Concentration, in: *Density and Viscosity*, *ASHRAE Trans* (1990), 1990, pp. 709-728

[20] ***, Engineering Analysis of Experimental Data – ASHRAE Guideline 2-1986., American Society of Heating, Refrigerating and Air-Conditioning Engineers, Inc., Atlanta, Ga., USA